IEEE Access
Multidisciplinary : Rapid Review : Open Access Journal

Received December 30, 2020, accepted January 6, 2021, date of publication January 11, 2021, date of current version January 22, 2021.

Digital Object Identifier 10.1109/ACCESS.2021.3050522

Spectrum-Sharing UAV-Assisted Mission-Critical Communication: Learning-Aided Real-Time Optimisation

MINH-HIEN T. NGUYEN[1], EMILIANO GARCIA-PALACIOS[1], TAN DO-DUY[2], LONG D. NGUYEN[3], (Member, IEEE), SON T. MAI[1], AND TRUNG Q. DUONG[1], (Senior Member, IEEE)

[1]Queen's University Belfast, Belfast BT7 1NN, U.K.
[2]Ho Chi Minh City University of Technology and Education, Ho Chi Minh City 700000, Vietnam
[3]Duy Tan University, Da Nang 550000, Vietnam

Corresponding author: Trung Q. Duong (trung.q.duong@qub.ac.uk)

This work was supported in part by the U.K. Royal Academy of Engineering (RAEng) under the RAEng Research Chair and the Senior Research Fellowship Scheme under Grant RCSRF2021\11\41, in part by the RAEng Research Fellowship Scheme under Grant RF1415\14\22. It was also supported in part by the Newton Fund Institutional Link through the Fly-by Flood Monitoring Project under Grant ID 428328486 and in part by Researcher Links grant, ID 527612186, under the Newton Fund partnership. The grants are funded by the UK Department for Business, Energy and Industrial Strategy and delivered by the British Council, for further information, please visit www.newtonfund.ac.uk. It was also supported in part by the Department for the Economy (DfE) under Global Challenges Research Fund (GCRF) scheme, NI DfE-GCRF 2020-2021.

ABSTRACT We propose an unmanned aerial vehicle (UAV) communications scheme with spectrum-sharing mechanism to provide mission-critical services such as disaster recovery and public safety. Specifically, the UAVs can serve as flying base stations to provide extended network coverage for the affected area under spectrum-sharing cognitive radio networks (CRNs). To cope with the effects of network destruction in a disaster, we propose a real-time optimisation framework for resource allocation (e.g., power and number of UAVs) for CRNs assisted by UAV relays. The proposed optimisation scheme aims at optimising the network throughput of primary and secondary networks under the stringent constraint of maximum tolerable interference impinged on the primary users. We also propose a deep neural network (DNN) model to significantly reduce the execution time under real-time solution of mixed-integer UAV deployment problems. For both primary and secondary networks, our real-time optimisation algorithms impose low computational complexity, hence, have a low execution time in solving throughput optimisation problems, which demonstrates the benefit of our approached proposed for spectrum-sharing UAV-assisted mission-critical services.

INDEX TERMS Real-time optimisation, unmanned aerial vehicle (UAV), spectrum sharing, machine learning, mission-critical communications.

I. INTRODUCTION

Future wireless networks, i.e., 5G and beyond, will not only enhance mobile broadband but also provide mission-critical communications with ultra-reliable and low latency communications (URLLC). In the event of a natural disaster, unmanned aerial vehicles (UAVs) play a significant role in search and rescue (SAR) missions [2]. The UAVs have to stay airborne above the affected area to aid first responders in assessing the gravity of the disaster as promptly as possible. Yet the UAVs' airborne duration is limited by their battery capacity [2], whereas SAR missions require intensive assistance from UAVs during the first hours of the disaster.

Additionally, the UAVs' operation is conventionally mandated in the unlicensed spectrum bands shared with other wireless technologies including the IEEE S-Band, IEEE L-Band, and ISM-Band. These bands are becoming more crowded due to the escalating proliferation of Internet-of-things devices and D2D communications. Hence, supporting the UAVs' operation in a cognitive radio network (CRN) becomes a promising technique of increasing the UAVs' available radio resources in addition to the unlicensed band. The integration of UAVs into spectrum-sharing networks has attracted substantial interest from the research

The associate editor coordinating the review of this manuscript and approving it for publication was Guangjie Han.

community [3]–[5]. In [3], the authors enhanced the spectrum sensing performance, by arranging for a UAV to perform spectrum sensing by circularly flying over the primary user (PU) with the objective of accessing the idle spectrum. By contrast, the UAV can also operate concurrently with the PU [4], where it acts as a relay to forward the messages from both the PU and SU to the designated receivers.

While combining a UAV with CRNs is capable of improving the spectral efficiency, there are several technical problems associated with UAV-aided communication. One of the most important issues is the UAV's energy consumption, which represents the main drawback of UAVs' applications [6], [7]. To address this, joint trajectory and power allocation optimisation has been conceived for UAV-CRNs in [6]. Given this transmission strategy, the average achievable rate of the UAV to SU link can be optimised subject to the UAV's speed, location and transmit power. Although the aforementioned contributions have shed light on the UAVs' application, especially on their suitability in disaster relief efforts, UAV-enabled communication is still facing limitations that should be addressed for ensuring the success of SAR missions. In particular, a prompt action is required of network controllers in support of UAV communications due to the dynamically changing environment [2], which is one of the most critical constraints in UAV applications. In all the UAV-aided optimisation scenarios found in the open literature [3]–[7] and the references therein, solving a convex optimisation problem can only be achieved after a long period of time, which is not particularly suitable for mission-critical services. Therefore, maximising the performance of UAV communication networks is vital for such applications.

In [8], the authors utilised UAVs as a solution to enhance the average secrecy rate in the cognitive communication networks, by optimising UAVs' robust trajectory and transmit power allocation. In [9], considering the downlink transmission of UAV-enabled networks in coexistence with D2D communication, the authors proposed a joint design of D2D assignment and resource allocation for maximising ground terminals throughput. In addition, in [10], the authors have formulated and solved the throughput maximisation problem, by jointly combining optimal location and spectrum sensing duration of the UAVs. However, the cognitive UAV network considered in [10] only consists of a single (primary) receiver, which is generally different from our model. Moreover, aiming at maximising a SU's throughput, the work in [11] studied the joint optimisation problem of the UAV placement and power allocation. However, [11] considered only a cognitive/secondary UAV transmitter communicating with the ground SU. Very recently, we have investigated the energy efficiency of UAV-CRNs in disaster recover scenarios in [1], [12], [13].

Against this background, we extend our previous work [1] by conceiving advanced optimisation techniques and training deep neural networks (DNNs). We propose a practical optimisation technique for enabling cognitive UAV communications to restore reliable network coverage in disaster-relief missions. Explicitly, joint execution time and throughput optimisation is conceived, which involves the deployment of UAVs under the control of mix-integer optimisation programming and robust resource allocation under throughput maximisation. The numerical results demonstrate the benefits of our approaches proposed for UAV-CRNs. The main contributions of this paper are as follows:

- We consider CRNs assisted by UAVs acting as relays, to cope with the network destruction in the event of a natural disaster. We then propose optimal resource allocation algorithms to maximise the throughput of primary and secondary networks under the rapid UAVs' deployment. Our model considers real-time optimisation in embedded UAV-CRN communication invoked for recovering wireless communication services.
- For the UAV deployment, an amalgamated optimisation and machine learning method relying on a DNN model is proposed for a significant reduction in the execution time under real-time solution of mixed-integer UAV deployment problems. This technique results in a learning-based optimisation programming which is associated with the connotation of "black box" optimisation.
- For the throughput maximisation of primary and secondary networks, we propose real-time optimisation algorithms to maximise the total throughput or guarantee the QoS fairness, i.e., maximise the worse-case scenario (PU or UAV) in the networks.
- All proposed optimal resource allocation algorithms have low-complexity for solving the non-convex throughput maximisation problem with rapid UAV deployment under both power budget and quality-of-service (QoS) constraints for dealing with the challenges of limited spectral and power resources in UAV systems. Our solutions become capable of supporting real-time applications in disaster recovery scenarios with low execution time in solving practical optimisation problems.

II. UAV-CRN SYSTEM AND CHANNEL MODEL

A. SYSTEM MODEL

We consider relay-assisted UAV in CRNs, where a macro base station (BS) is equipped with a massive multiple-input multiple-output (MIMO) array. Here, the N transmit antennas (TAs) at the BS are utilised to serve K_P primary users (PUs) located in the primary network (safety area). Meanwhile, in the secondary network (disaster area), the UAVs are deployed as small-cell flying base stations, which can be connected to the cellular networks via the BS; the aim is to restore reliable wireless network(s) operation in the hazardous areas and to serve as many SUs in the disaster region as possible. All SUs that are served are represented by M groups given by the set of $\mathcal{K}_S = \{\mathcal{K}_1, \dots, \mathcal{K}_M\}$, which are supported by the set of UAVs $\mathcal{M} = \{1, \dots, M\}$ required

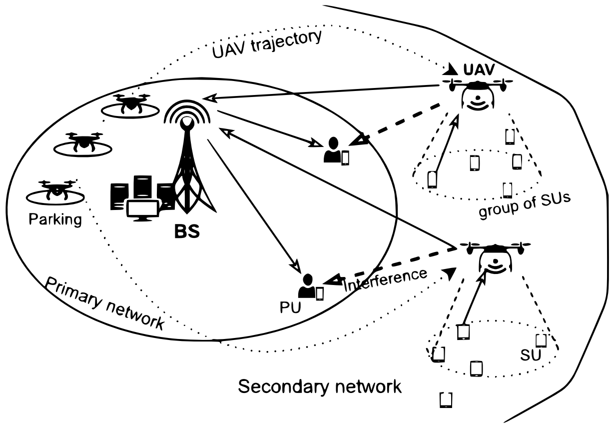

FIGURE 1. A model of UAV-enabled cognitive small cell network in disaster relief.

for restoring reliable network operation. We set the number of PUs and SUs to $\mathcal{K}_P = \{1, \ldots, K_P\}$ and $\mathcal{K}_S = \{1, \ldots, K_S\}$, respectively. Both the PUs and SUs are randomly distributed in the primary and secondary networks constituted by the set of $\mathcal{K} = \{\mathcal{K}_P, \mathcal{K}_S\}$. The deployment and trajectory design of the UAVs is controlled by the terrestrial BS as shown in Fig. 1. Apart from the BS, all other terminals are single-antenna equipped.

B. CHANNEL MODEL

We define the 3D location of the BS, the UAVs and of all the users (PUs and SUs) as (x_0, y_0, H_0), (x_m, y_m, H_m), $m \in \mathcal{M}$ and $(x_k, y_k, 0)$, $k \in \mathcal{K}$, respectively. The antenna heights of the BS and the UAV are respectively denoted as H_0 and H_m. We assume a UAV's antenna altitude is also its altitude. These locations are determined by using the Global Positioning System (GPS) and stored at the ground station.

Due to the line-of-sight (LoS) propagation and the 3D nature of UAV-enabled communications, we can exploit the air-to-air (ATA) link to enhance the BS-UAV links explicitly as LoS propagation is highly likely to occur in the ATA links. Hence, the path loss between the BS and the mth UAV follows the free-space path loss model as [12], [14]

$$\beta_{0,m} = \frac{\beta_0}{d_{0,m}^2 + (H_0 - H_m)^2}, \quad m = 0, 1, \ldots, M \tag{1}$$

where β_0 is the channel's power gain at reference distance d_0 and $d_{0,m} = \sqrt{(x_0 - x_m)^2 + (y_0 - y_m)^2}$.

By contrast, the air-to-ground (ATG) channels are more complex due to the effects of propagation blockage such as shadowing, blockage geometry and disaster paraphernalia. The path-loss expression between the mth BS and the kth user is denoted as [15]

$$\beta_{m,k} = PL_{m,k} + \eta_{LoS} P_{m,k}^{LoS} + \eta_{NLoS} P_{m,k}^{NLoS} \tag{2}$$

where η_{LoS} and η_{NLoS} are the average additional losses for the LoS and NLoS paths, respectively. Here, the distance-related path loss is given by

$$PL_{m,k} = 10 \log \left(\frac{4\pi f_c R_{m,k}}{c} \right)^{\alpha} \tag{3}$$

where f_c is the carrier frequency (Hz), c is the speed of light (m/s), and $\alpha \geq 2$ is the path loss exponent. The probability of LoS is given by [16]

$$P_{m,k}^{LoS} = \frac{1}{1 + a \exp\left[-b \left(\arctan\left(\frac{H_m}{d_{m,k}} \right) - a \right) \right]} \tag{4}$$

where a and b are constants, depending on the environment. Then, we have $P_{m,k}^{NLoS} = 1 - P_{m,k}^{LoS}$. Finally, we can rewrite (2) as

$$\beta_{m,k} = 10\alpha \log(R_{m,k}) + A \times P_{m,k}^{LoS} + B \tag{5}$$

where $A = \eta_{LoS} - \eta_{NLoS}$, $B = PL_{m,k} + \eta_{NLoS}$, and $R_{m,k}$ denotes the distance between the mth BS and the kth user, formulated as

$$R_{m,k} = \sqrt{d_{m,k}^2 + H_m^2}, \; k \in \mathcal{K} \tag{6}$$

where $d_{m,k} = \sqrt{(x_m - x_k)^2 + (y_m - y_k)^2}$ is the Euclidean distance between the mth UAV and the kth user.

C. TRANSMISSION SCHEME

1) PRIMARY NETWORK

Let us consider the transmission in the primary network where the BS transmits its signal to the PUs. Firstly, the signal received at the kth PU ($k \in \mathcal{K}_P$) is given by

$$y_{0,k} = \underbrace{\sqrt{P_0} \mathbf{g}_{0,k}^T \boldsymbol{f}_{0,k} s_{0,k}}_{\text{desired signal}} + \underbrace{\sum_{k' \in \mathcal{K}_P \setminus \{k\}} \sqrt{P_0} \mathbf{g}_{0,k}^T \boldsymbol{f}_{0,k'} s_{0,k'}}_{\text{co-tier interference}} + \underbrace{\sum_{l=1}^{M} g_{l,k} \sqrt{P_l} s_{l,0}}_{\text{inter-cell interference}} + n_k \tag{7}$$

where P_0 is the transmit power of the BS; $\mathbf{g}_{0,k} \in \mathbb{C}^N$ is the channel coefficients between the BS and kth PU; $\boldsymbol{f}_{0,k} \in \mathbb{C}^N$ and $s_{0,k} \in \mathbb{C}$ are the beamforming vector and the information transmitted from the BS with $||s_{0,k}||^2 \leq 1$. Here, we utilise the structure of the ATA links by including both large-scale and small-scale fading effects as $\mathbf{g}_{0,k} = \sqrt{\beta_{0,k}} \boldsymbol{h}_{0,k}$, where $\boldsymbol{h}_{0,k}$ is the small-scale fading coefficients for channels from BS to kth PU. Moreover, P_l is the transmit power of the lth UAV; $n_k \sim \mathcal{CN}(0, \sigma_k^2)$ is the additive white Gaussian noise (AWGN). To elaborate the right-hand side of (7), the first term is the desired signal designated for the kth PU, the second term is the co-tier interference from the remaining PUs, and the last term is the inter-cell interference from the UAVs in the secondary network.

In this paper, for the massive MIMO BS, we employ efficient maximal ratio transmission (MRT) criterion in beamforming design for the massive MIMO array at the BS, which is formulated as follows [17]:

$$\boldsymbol{f}_{0,k} = \sqrt{p_{0,k}} \frac{\boldsymbol{g}^*_{0,k}}{\|\boldsymbol{g}_{0,k}\|} \tag{8}$$

where $p_{0,k}$ is the power control coefficient. Then, we introduce $\rho_{0,k,j} = \boldsymbol{g}^T_{0,k}\boldsymbol{g}^*_{0,j}/\|\boldsymbol{g}_{0,j}\|$.

For the power control coefficients $\boldsymbol{p}_0 = [p_{0,k}]_{k\in\mathcal{K}_P}$ and $\boldsymbol{p}_M = [P_m]_{m\in\mathcal{M}}$, the network interference imposed on the primary network is characterised by the co-tier interference formulated as

$$\mathcal{I}^{\text{intra}}_k(\boldsymbol{p}_0) = P_0 \sum_{k'\in\mathcal{K}_P\setminus\{k\}} p_{0,k'}|\rho_{0,k,k'}|^2, k \in \mathcal{K}_P \tag{9}$$

and the inter-cell interference inflicted by the secondary network[1]

$$\mathcal{I}^{\text{inter}}_k(\boldsymbol{p}_M) = \textstyle\sum_{m\in\mathcal{M}} P_m|\beta^{atg}_{m,k}|^2, k \in \mathcal{K}_P. \tag{10}$$

The information throughput of the kth PU (in nats) is given by

$$R_{0,k}(\boldsymbol{p}_0, \boldsymbol{p}_M) = \ln\left(1 + \frac{P_0\, p_{0,k}|\rho_{0,k,k}|^2}{\mathcal{I}^{\text{intra}}_k(\boldsymbol{p}_0) + \sigma^2_k}\right). \tag{11}$$

To ensure the quality-of-service (QoS) of the primary network, the QoS constraints have to be investigated in the face of inter-cell interference

$$\mathcal{I}^{\text{inter}}_k(\boldsymbol{p}_M) \le I^{PU}_{th} \tag{12}$$

where I^{PU}_{th} is the maximum tolerable interference still capable of ensuring the QoS of the PUs.

Thus, the total throughput of the primary network is expressed as

$$R_{pri}(\boldsymbol{p}_0, \boldsymbol{p}_M) = \sum_{k\in\mathcal{K}_P} R_{0,k}(\boldsymbol{p}_0, \boldsymbol{p}_M). \tag{13}$$

2) SECONDARY NETWORK

Simultaneously, we consider the transmission in the secondary network where the UAVs also forward the signals from the SUs to the BS. The signal received at the BS from the mth UAV is written as

$$y_{m,0} = \underbrace{\boldsymbol{g}^T_{m,0}\boldsymbol{f}_{m,0}\sqrt{P_m}s_{m,0}}_{\text{desired signal}} + \underbrace{\sum_{l=1,l\neq m}^{M} \boldsymbol{g}^T_{m,0}\boldsymbol{f}_{l,0}\sqrt{P_l}s_{l,0}}_{\text{inter-cell interference}} + n_0 \tag{14}$$

where P_m is the transmit power of the mth UAV; $\boldsymbol{g}_{m,0}$ is the channel coefficients between the mth UAV and BS; $\boldsymbol{f}_{m,0}$ is transmit beamforming vector and $s_{m,0}$ is information transmitted by the mth UAV with $||s_{m,0}||^2 \le 1$, $n_0 \sim \mathcal{CN}(0, \sigma^2_0)$ is the AWGN.

Similar to (8), we apply MRT for the transmission of the secondary network and we also introduce $\rho_{m,0,l} = \boldsymbol{g}^T_{m,0}\boldsymbol{g}^*_{l,0}/\|\boldsymbol{g}_{l,0}\|$.

[1] It is very hard to estimate the ATG channel between UAVs and PUs, so the inter-cell interference from the secondary network can only be estimated by the UAVs and determined as in (10).

The information throughput of the BS (in nats) received by the mth UAV can be written as

$$R_{m,0}(\boldsymbol{p}_M) = \ln\left(1 + \frac{P_m|\rho_{m,0,m}|^2}{\mathcal{I}^{\text{BS}}_m(\boldsymbol{p}_M) + \sigma^2_0}\right) \tag{15}$$

where $\mathcal{I}^{\text{BS}}_m(\boldsymbol{p}_M) = \sum_{l\in\mathcal{M},l\neq m} P_l|\rho_{m,0,l}|^2$ represents the inter-cell interference imposed on the BS.

Thus, the total throughput of the secondary network is expressed as the total throughput of all UAVs

$$R_{sec}(\boldsymbol{p}_M) = \sum_{m\in\mathcal{M}} R_{m,0}(\boldsymbol{p}_M). \tag{16}$$

D. PROBLEM FORMULATION

In this paper, our main target is to maximise the network throughput of either the primary or secondary network by using BS association and power allocation optimisation for CRNs assisted by UAVs. Hence, we define two optimisation problems: the maximisation of the primary network throughput (MaxPRI) and the maximisation of the secondary network throughput (MaxSEC). The corresponding optimisation problems are respectively formulated as

$$\text{Problem I}: \max_{\boldsymbol{p}_0, \boldsymbol{p}_M, (m,k)} R_{pri}(\boldsymbol{p}_0, \boldsymbol{p}_M) \tag{17a}$$

$$\text{s.t.} \sum_{k\in\mathcal{K}_P} p_{0,k} \le 1, P_m \le P^{\max}_m, m \in \mathcal{M}, \tag{17b}$$

$$R_{m,0}(\boldsymbol{p}_M) \ge \bar{r}_{m,0},\ m \in \mathcal{M}, \tag{17c}$$

$$R_{0,k}(\boldsymbol{p}_0, \boldsymbol{p}_M) \ge \bar{r}_{0,k},\ k \in \mathcal{K}_P, \tag{17d}$$

$$(m, k) \in \mathcal{K}_m, m \in \mathcal{M},\ k \in \mathcal{K}_m, \tag{17e}$$

$$\text{Problem II}: \max_{\boldsymbol{p}_0, \boldsymbol{p}_M, (m,k)} R_{sec}(\boldsymbol{p}_M) \tag{18a}$$

$$\text{s.t. (17b)} - \text{(17e)}, \tag{18b}$$

where the constraint (17b) represents the power requirements at the UAVs and the BS, while the constraints (17c) and (17d) formulate the QoS requirement of the UAV-BS and BS-PU links, respectively. The constraint (17e) corresponds to the deployment of the UAVs at the beginning. We set $\mathcal{K}_m = \{1, \ldots, K_m\}$ and $\sum_{m\in\mathcal{M}} K_m = K_S$.

Obviously, the problems (17)-(18) are non-convex problems with the non-convex functions of (17a), (17c)-(17e), and (18a). Moreover, when large-scale scenarios are considered, the problems become very complex due to the large number of UAVs (M) and users in the deployment area. For efficiently solving the non-convex problems (17)-(18), we separate the two problems into two subproblems. Firstly, the user association with UAV clustering will be proposed that will satisfy constraint (17e) under the deployment of UAVs. Then, a DNN is applied for constructing the optimisation strategy of UAV deployment for the real-time context considered. Finally, the optimal power is assigned for maximising the network throughput given QoS requirements.

III. LEARNING OPTIMISATION FOR A REAL-TIME SCENARIO OF UAV DEPLOYMENT

A. CONVENTIONAL OPTIMISATION APPROACH FOR UAV DEPLOYMENT

In order to guarantee the QoS of ATG links between UAVs and users, we consider the coverage region by defining a circular disc of radius D_{cov}. The radius $D_{m,cov}$ is related to the altitude of UAV m as follows:

$$H_m = D_{m,cov} \tan(\theta), \forall m, \tag{19}$$

where θ is set to 42.44° [18]. Therefore, a SU can be served by a UAV in its coverage area $(m, k) \in \mathcal{K}_m$ if the Euclidean distance between the UAV and the SU is less than the coverage distance $D_{m,cov}$, which is formulated as

$$d_{m,k} \leq D^{max}_{m,cov}\ k \in \mathcal{K}_S, \tag{20}$$

where $D^{max}_{m,cov} = H^{max}_m / \tan(\theta)$.

Given the limited operational range of the UAV, we formulate a UAV positioning optimisation problem to provide a best-effort transmission service for the secondary network in each group

$$\max_{\boldsymbol{q}_m, u_{m,k}} \sum_{m=1}^{M} \sum_{k=1}^{K_m} u_{m,k} \tag{21a}$$

$$\text{s.t. } d^2_{m,k} \leq (D^{max}_{m,cov})^2 + \lambda_m(1 - u_{m,k}), \tag{21b}$$

$$\boldsymbol{q}_m \in [\boldsymbol{q}^{\min}_m, \boldsymbol{q}^{max}_m], \tag{21c}$$

$$u_{m,k} \in \{0, 1\}, \tag{21d}$$

$$m \in \mathcal{M},\ k \in \mathcal{K}_m,$$

where $\boldsymbol{q}_m = [x_m, y_m, H^{max}_m]^T$, λ_m is chosen as a specific value corresponding to the maximum network coverage area of the mth UAV (i.e., $\lambda_m > (D^{max}_{m,cov})^2$), while (x_{min}, x_{max}) and (y_{min}, y_{max}) represent the lower and upper bounds of the horizontal and vertical range of UAVs, respectively. Note that the problem in (21) is a mixed-integer (binary) quadratic programming, which is non-convex problem. Solving the above problem, which belongs to combinatorial (or discrete) optimisation, is often very difficult. Fortunately, the Python-embedded optimisation program CVXPY [19] by using an appropriate solver is capable of solving problem (21).

Although conventional optimisation for UAV deployment relying on the CVXPY platform for example can solve problem (21), the execution time imposed by solving the related mixed-integer program in excessive, when the networking scenario becomes more complex and when the number of integer variables $(u_{m,k})$ increases. The problem (21) is one of the most complex problem with the worst-case complexity up to $\mathcal{O}(2^{mk})$ where m and k are the number of UAVs and SUs, respectively. There are approaches to reducing the computational complexity of combinatorial algorithms for solving this kind of problems such as exhaustive search, evolution algorithm or genetic algorithms. As a result, we will propose a new optimisation algorithm for UAVs deployment using a DNN for learning optimisation in the next sub-section.

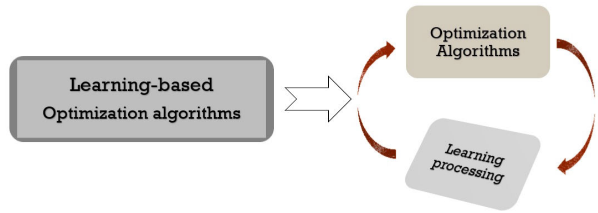

FIGURE 2. A model of learning-based optimisation algorithm by using DNN.

B. DEEP NEURAL NETWORK FOR LEARNING OPTIMISATION OF UAV DEPLOYMENT

Where existing optimisation algorithms might be infeasible, the collaboration of machine learning and optimisation offers simple and efficient techniques in dealing with NP-problems [20]–[22], and complex and large-scale optimisation problems in real-time applications. In this regard, DNN [23], [24] is an efficient machine learning approach that can be applied in real-time optimisation methods.

In particular, to tackle the aforementioned problem, we apply a new optimisation technique eminently suitable for real-time applications by amalgamating DNN and optimisation algorithms. This technique results in learning-based optimisation programming [21], as presented in Fig. 2. Deep learning is a technique from computational procedure over successive iterations. It is used to build an approximation of the objective function and guide the good choice made in the next iteration. DNN models can estimate the outcome of a series of sub-problems all at once, attempt to reduce the complexity of a constrained continuous optimisation problem by shrinking the solution space using a feature selection technique, and adjust metaheuristic solution methods for multi-objective optimisation, e.g, choosing appropriate heuristic methods or finding initial solutions. In fact, DNN stands for the development of algorithms or techniques that learn from observed data by assembling mathematical models. A fully connected DNN model consists of three types of layers including one input layer, one (or multiple) hidden layer(s) and one output layer.

In this context, a learning-based approach is proposed for the optimisation of wireless networks in [21]. Following the system setup in [21], we configure the network structure for our DNN model as follows:

- The input of the network is the location of the UAVs and SUs $(\boldsymbol{q}_m, \boldsymbol{q}^{SU}_k)$, while the output of the network is the optimal value of $\boldsymbol{q}^*_m$. In all the layers, we use "sigmoid" $f(x) = \frac{1}{1+e^{-x}}$ as the activation function.
- Activation functions are an important feature of DNN. They decide whether a node in the layer, which is receiving information relevant to the given information, should be activated or not:
  $Y = \text{activation}(\sum(\text{weight} * \text{input}) + \text{bias})$
- In the testing stage, we use a large training data set $(\boldsymbol{q}_m, \boldsymbol{q}^{SU}_k)$ for optimising and learning the weights of

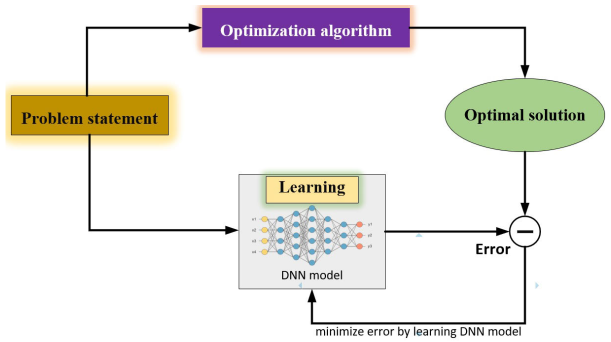

FIGURE 3. A DNN-based approach to learn optimisation algorithm via minimising the error of solution between conventional algorithm and DNN model.

the DNN model. The cost function (CF) is the mean squared error (MSE) and the mini-batch stochastic gradient descent (SGD) optimisation algorithm is used [21].

- In the testing stage, we also generate the structure based on the same distribution during the training stage. Each distributed location experiment is passed through the trained network and then we collect the resultant optimal location of the UAVs.

Explicitly, the optimisation algorithms will be trained for learning the input/output relationship by using a DNN model during the training stage. Several network layers will approximate a training set of resource management algorithms by using a DNN model, which requires simple operations to implement a finite training sample set. With the aid of sufficient training data set, their optimisation technique is capable of completely replacing the conventional optimisation processes during the testing stage.

As shown in Fig. 3, if the learning-based optimisation algorithm learns the updated formula, it can learn a new algorithm that is modelled as a neural network. Learning the weights of the neural network and parameterising the updated formula of the algorithm can provide useful function approximators, model any updated formula with sufficient capacity, allow for efficient search and easily perform training process with backpropagation. Therefore, the appropriate optimiser would simply memorise the optimum, and after learning with sufficient training set, the optimiser then converges to the optimum within a few steps regardless of initialisation in the future.

IV. MAXIMISING NETWORK THROUGHPUT VIA ROBUST POWER ALLOCATION

After solving the UAV deployment problem, in this section, we conceive efficient resource allocation for solving the network throughput maximisation problems (17)-(18) in the absence of non-convex user association constraints ($u_{m,k}$). On the other hand, the problems (17)-(18) are still non-convex ones since the objective functions are non-concave. Hence, we consider the modified problems as

$$\text{Problem I} - \text{B}: \max_{\boldsymbol{p}_0, \boldsymbol{p}_M} R_{pri}(\boldsymbol{p}_0, \boldsymbol{p}_M) \tag{22a}$$

$$\text{s.t. } (17\text{b}) - (17\text{d}). \tag{22b}$$

$$\text{Problem II} - \text{B}: \max_{\boldsymbol{p}_0, \boldsymbol{p}_M} R_{sec}(\boldsymbol{p}_M) \tag{23a}$$

$$\text{s.t. } (17\text{b}) - (17\text{d}). \tag{23b}$$

To solve problems (22)-(23), we use some efficient approximation and logarithm inequalities [25] (see Appendix A for detailed proofs).

Hence, at the ith iteration, the following convex programs are solved to generate the feasible points:

$$\text{Problem I} - \text{C}: \max_{\boldsymbol{p}_0, \boldsymbol{p}_M} \hat{R}^{(i)}_{pri}(\boldsymbol{p}_0, \boldsymbol{p}_M) \tag{24a}$$

$$\text{s.t. } \sum_{k \in \mathcal{K}_P} p_{0,k} \leq 1, P_m \leq P_m^{\max}, m \in \mathcal{M}, \tag{24b}$$

$$\hat{R}^{(i)}_{m,0}(\boldsymbol{p}_M) \geq \bar{r}_{m,0}, \; m \in \mathcal{M}, \tag{24c}$$

$$\hat{R}^{(i)}_{0,k}(\boldsymbol{p}_0, \boldsymbol{p}_M) \geq \bar{r}_{0,k}, \; k \in \mathcal{K}_P, \tag{24d}$$

$$\text{Problem II} - \text{C}: \max_{\boldsymbol{p}_0, \boldsymbol{p}_M} \hat{R}^{(i)}_{sec}(\boldsymbol{p}_M) \tag{25a}$$

$$\text{s.t. } (24\text{b}) - (24\text{d}), \tag{25b}$$

where $\hat{R}^{(i)}_{pri}(\boldsymbol{p}_0, \boldsymbol{p}_M) = \sum_{k \in \mathcal{K}_P} \hat{R}^{(i)}_{0,k}(\boldsymbol{p}_0, \boldsymbol{p}_M)$ and $\hat{R}^{(i)}_{sec}(\boldsymbol{p}_M) = \sum_{m \in \mathcal{M}} \hat{R}^{(i)}_{m,0}(\boldsymbol{p}_M)$, the form of $\hat{R}^{(i)}_{m,0}(\boldsymbol{p}_M)$ and $\hat{R}^{(i)}_{0,k}(\boldsymbol{p}_0, \boldsymbol{p}_M)$ are defined by (31) and (29), respectively.

We now proceed by proposing an algorithm to solve the proposed throughput maximisation problems. In Algorithm 1, we propose a power allocation procedure for solving problem (24). The initial point $(\boldsymbol{p}_0^{(0)}, \boldsymbol{p}_M^{(0)})$ for (24) may be found by random search for a point satisfying the constraints (24b)-(24d). The power allocation procedure for solving problem (25) is similar to Algorithm 1.

Algorithm 1 : Power Allocation Procedure for Solving Problem (24)

Input:
Set M, K_m, K_p, P_0, P_m
Set the tolerance $\varepsilon = 10^{-2}$ or the maximum number of iterations $I_{max} = 20$ to stop the algorithm.
Set $i = 0$ and a feasible point.
Repeat
Solve problem (24) for the optimal solution $(\boldsymbol{p}_0^{(i+1)}, \boldsymbol{p}_M^{(i+1)})$
Set $i := i + 1$
Until Convergence of the objective function in (24) or $i > I_{max}$.
Output: Optimal power control coefficients $(\boldsymbol{p}_0, \boldsymbol{p}_M)$

V. SIMULATION RESULTS

In this section, the performance of the considered system is evaluated by using embedded optimisation programming, such as for example the CVXPY version 1.0.21 in

Python [19]. The computational platform includes a PC having a AMD Ryzen 7 2700X, CPU @3.7GHz and 32GB memory. Our DNN model was implemented in Python 3.6 associated with Keras 2.2.4 using TensorFlow 1.13.1.

A. SIMULATION SETTINGS

We set the system parameters for our simulations as follows:

- The safety area is a circle coverage with a radius of 500m,
- The disaster area is extended from the safety area with a radius up to 2000m,
- The location of the BS is assumed at (0, 0, 30) while PUs and SUs are randomly distributed in the primary network and secondary network, respectively,
- The path loss from BS to PUs is as $\beta_{0,k}^{atg} = 148.1 + 37.6\log_{10} R$ [dB], R in km,
- The number of UAVs is provided as $M = \{4, 8\}$. The number of PUs is set to $K_P = \{10, 20, 30, 60\}$ while the number of SUs in each group is set to $K_m = \{20, 30\}$,
- The limited altitude of the UAVs (H^{min}, H^{max}) is (50, 150)m,
- The tolerance and maximum number of iterations for convergence of algorithms are $\varepsilon = 10^{-3}$ and $I_{max} = 10$,
- The carrier frequency / bandwidth is $f_c = 2$ GHz / $B = 10$ MHz,
- The QoS thresholds are set to $\bar{r}_{m,0} = 40$ Mbps and $\bar{r}_{0,k} = 1$ Mbps,
- The maximum transmit power is set to 40W and 5W for BS and UAVs, respectively,
- The white power spectral density is $\sigma^2 = -130$ dBm/Hz.

The parameters of the channel model are set as in [14], [18], [25].

B. NUMERICAL RESULTS

The numerical results are conducted from our proposed approaches, i.e., MaxPRI in (22) and MaxSEC in (23) and the two conventional methods to guarantee the QoS fairness among the primary and secondary networks. More particularly, four different cases are generated from the following algorithms:

- Primary network throughput maximisation (MaxPRI): maximising the throughput of primary network as in (22).
- Secondary network throughput maximisation (MaxSEC): maximising the throughput of secondary network as in (23).
- Maximisation of minimum primary network throughput(MaxMinPRI): maximising the worst-case PU throughput, i.e., $\max\limits_{p_0,p_M,(m,k)} \min\limits_{k\in\mathcal{K}_P} R_{0,k}(p_0, p_M)$, under the same constraints as Problem I-A. Here, the worst-case PU throughput is defined as the average throughput (in nats) of the PU with the lowest throughput in the primary network.

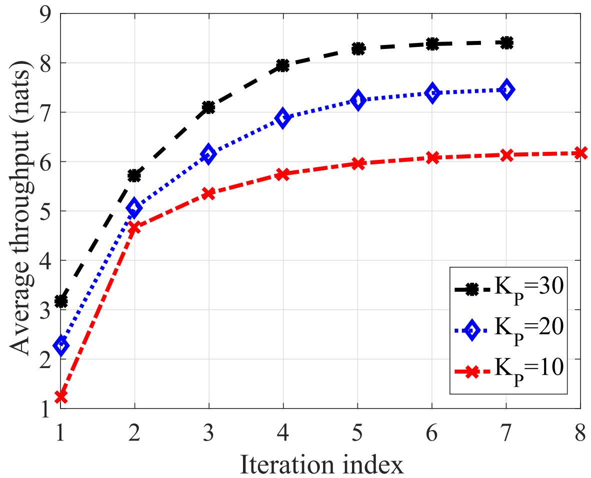

FIGURE 4. The convergence of Algorithm 1 for solving Problem I-C (MaxPRI) at $M = 4$, $K_m = 20$, $P_m = 35$ dBm.

- Maximisation of minimum secondary network throughput (MaxMinSEC): maximising the worst-case UAV throughput, i.e., $\max\limits_{p_0,p_M,(m,k)} \min\limits_{m\in\mathcal{M}} R_{m,0}(p_M)$, under the same constraints as Problem II-A. Here, the worst-case UAV throughput is defined as the average throughput (in nats) of the UAV with the lowest throughput in the secondary network.

For the sake of fairness, in all the four algorithms, we evaluate the average total throughput (in nats) of all the PUs and UAVs in the system, i.e., $R_{pri}(p_0, p_M) + R_{sec}(p_M)$. More specifically, in each figure, four different curves are generated as follows:

- MaxPRI: the total throughput of both primary and second networks are plotted where we only optimise the throughput of the **primary network** as in (22) and the throughput of the secondary network are set not to fall below its QoS constraint.
- MaxSEC: the total throughput of both primary and second networks are plotted where we only optimise the throughput of the **secondary network** as in (23) and the throughput of the primary network are set not to fall below its QoS constraint. In addition, while we optimise the secondary network, the maximum tolerable interference impinged on the PUs is also satisfied as in (12).
- MaxMinPRI: the total throughput of both the primary and second networks are plotted where we only maximise the worst-case PU throughput.
- MaxMinSEC: the total throughput of both the primary and second networks are plotted where we only maximise the worst-case UAV throughput.

1) CONVERGENCE OF ALGORITHMS

Figure 4 illustrates the convergence of Algorithm 1 for solving Problem I-C (MaxRatePri) at $M = 4$, $K_m = 20$, $P_m = 35$ dBm. It is observed that after a few iterations, the objective function (24a) converges to its maximum value.

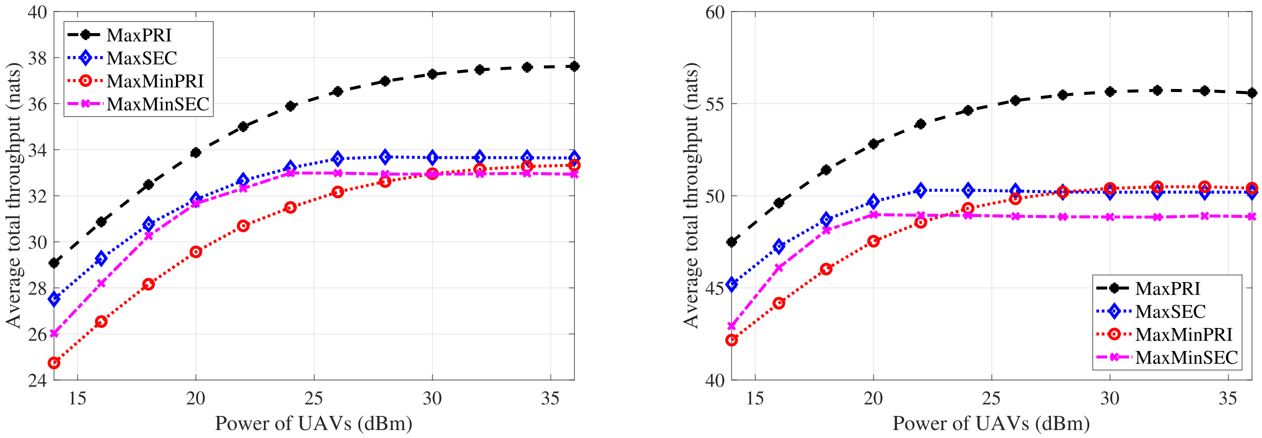

(a) $M = 4$, $K_m = 20$ (b) $M = 8$, $K_m = 30$

FIGURE 5. **Average total network throughput versus the power of UAVs (P_m) with $K_p = 60$.**

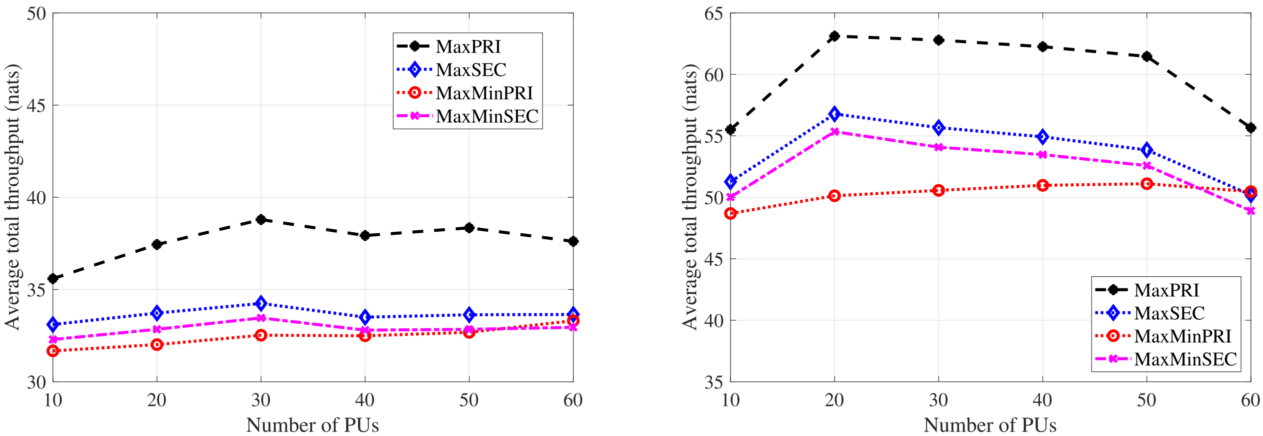

(a) $M = 4$, $K_m = 20$ (b) $M = 8$, $K_m = 30$

FIGURE 6. **Average total network throughput versus number of PUs (K_p) with $P_m = 35$ dBm.**

2) OPTIMAL TOTAL THROUGHPUT VERSUS THE POWER OF UAVs

In Figure 5, we show the average total network throughput as a function of the UAV's power (P_m) for the proposed throughput maximisation problems. Our major findings are as follows:

- As expected, the total network throughput with MaxPRI outperforms the others, demonstrating the efficiency of the power allocation with primary network throughput maximisation. Moreover, while MaxPRI and MaxSEC find optimal solutions to maximise the sum of network throughput, MaxMinPRI and MaxMinSEC only optimise either the PU or UAV with the worst throughput. Therefore, MaxPRI and MaxSEC obviously provide a better total throughput than those of MaxMinPRI and MaxMinSEC.
- For the considered schemes taking into account the secondary network throughput maximisation, the total network throughput increases with the power of UAVs until reaching a threshold (e.g., approximately $P_m = 25$ dBm and $P_m = 20$ dBm in the case of $M = 4$, $K_m = 20$ and $M = 8$, $K_m = 30$, respectively). As observed from Figures 5a and 5b, the higher the number of UAVs, the lower the P_m threshold above which the network throughput does not increase anymore. This is because the inter-cell interference caused by the UAVs increases significantly with a large number of UAVs.

3) OPTIMAL THROUGHPUT VERSUS THE NUMBER OF PUs

Figure 6 plots the average total throughput versus different number of PUs in the primary network considering different number of UAVs. We can observe from the figure that

- The average total network throughput goes up when the number of PUs is sufficiently small e.g., $K_P \leq 30$. However, the total throughput would reduce with larger number of PUs due to the co-tier interference in the primary network.
- As expected, given a particular UAV power, more UAVs are associated with higher the average total throughput of the network.

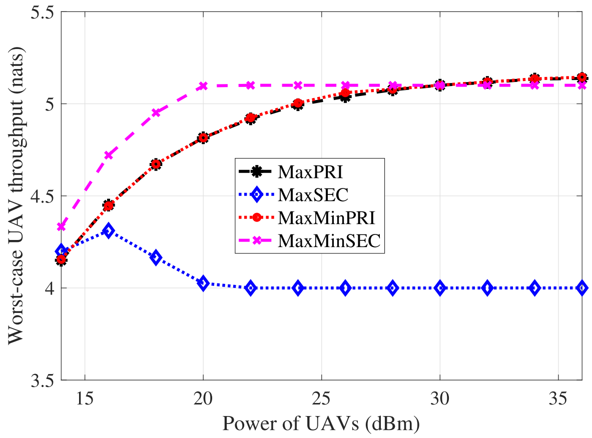

FIGURE 7. Worst-case UAV throughput versus UAV power at $M = 8$, $K_m = 30$, $K_P = 60$.

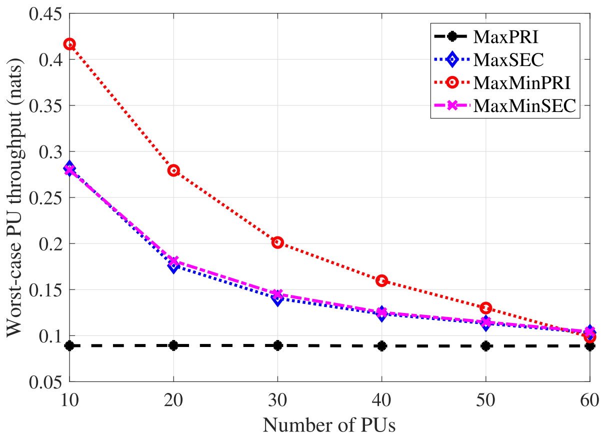

FIGURE 8. Worst-case PU throughput versus the number of PUs at $M = 8$, $K_m = 30$, $P_m = 35$ dBm.

4) THE WORST-CASE UAV AND PU THROUGHPUT

Figure 7 denotes the worst-case UAV throughput versus a range of UAV power at $M = 8$, $K_m = 30$, $K_p = 60$ for different power allocation schemes. We can see that

- By maximising the throughput of the UAV with the worst performance, MaxMinSEC outperforms the other schemes in terms of the worst-case UAV throughput. On the other hand, MaxSEC obtains lowest performance due to the fact that it only focuses on maximising the total throughput of the secondary network.
- Moreover, as mentioned above, the worst-case UAV throughput is limited by the inter-cell interference when the power of the UAVs, P_m, is large enough, especially in the case of MaxSEC.

In Figure 8, we evaluate the worst-case PU throughput for a range of different number of PUs.

- MaxMinPRI provides the highest worst-case PU throughput in comparison to the others because its objective function is to maximise throughput of the worst-case PU.
- Moreover, the larger the number of PUs, the higher the co-tier interference which reduces the PU throughput.

TABLE 1. The execution time of our UAV deployment algorithm both under conventional optimisation (Conv_UAV_Dep) and learning-aided optimisation using DNN model (DNN_UAV_Dep).

Scenarios $\{M, K_P, K_m\}$	Conv_UAV_Dep	DNN_UAV_Dep	Accuracy (%)
$\{2, 5, 10\}$	0.15s	0.027s	93.02
$\{4, 10, 20\}$	0.80s	0.028s	92.37
$\{8, 20, 30\}$	4.27s	0.028s	90.82

TABLE 2. The execution time of proposed optimisation algorithms for optimising network throughput performance.

Scenarios $\{M, K_m, K_P\}$	MaxPRI (ms)	MaxSEC (ms)	MaxMinPRI (ms)	MaxMinSEC (ms)
$\{4, 20, 10\}$	115	125	75	100
$\{4, 20, 30\}$	260	280	135	220
$\{4, 20, 60\}$	600	670	340	460
$\{8, 30, 10\}$	115	120	100	120
$\{8, 30, 30\}$	280	280	180	250
$\{8, 30, 60\}$	630	750	450	660

5) AVERAGE EXECUTION TIME FOR SOLVING OPTIMISATION PROBLEMS

In Table 1, we provide the average execution time for solving the UAV deployment problem via two proposed methods, i.e., conventional UAV deployment (Conv_UAV_Dep) and deep learning UAV deployment (DNN_UAV_Dep) schemes. The accuracy metric is defined by the difference from the values achieved in Conv_UAV_Dep and DNN_UAV_Dep to optimise the UAV deployment. The figures demonstrate the potential of learning-based optimisation algorithm by using the DNN model. As seen from Table 1, our proposed learning-aided UAV deployment procedure exhibits a low complexity and high accuracy, even upon dealing with large-scale scenarios.

As shown in Table 2, the average execution time for solving optimisation problems under sum rate maximisation and maximin worst-case rate in both primary and secondary networks is provided. All simulation results are consumed within milliseconds for up to 100 devices considered in the system.

VI. CONCLUSION

In this paper, a spectrum-sharing UAV communication scheme was conceived for establishing network coverage for mission-critical services, e.g., in the event of a natural disaster recovery. We proposed a novel learning-aided optimisation scheme for optimal radio resource allocation of the considered networks under the stringent constraint of maximum tolerable interference. By employing the deep learning approach, the UAVs deployment, i.e., the number of UAVs to serve the secondary users, can be quickly established. We then developed the real-time optimisation algorithms to optimise the throughput for both primary and secondary networks. Our low-complexity algorithms lend themselves to real-time deployment in the context of cognitive radio networks relying on UAVs. The numerical results demonstrated that our UAV deployment can be promptly optimised in a large-scale scenario. The proposed schemes revealed a compelling installation of real-time optimisation in wireless communication systems that have been destroyed by natural disasters. Through the numerical results, we have demonstrated the feasibility of the propose real-time optimisation which is computationally applicable with just a small amount of time needed for solving on a millisecond time-scale.

APPENDIX
APPROXIMATION APPROACHES AND INEQUALITIES USED TO SOLVE THE OPTIMISATION PROBLEMS (22) AND (23)

To solve problems (22) and (23), we exploit the logarithmic inequality of [25], [26], which follows from the convexity of the function $f(x, y) = \ln\left(1 + 1/xy\right)$, yielding

$$f(x, y) = \ln(1 + \frac{1}{xy}) \geq \hat{f}(x, y), \tag{26}$$

where we have

$$\hat{f}(x, y) = \ln\left(1 + \frac{1}{\bar{x}\bar{y}}\right) + \frac{2}{(\bar{x}\bar{y} + 1)} - \frac{x}{\bar{x}(\bar{x}\bar{y} + 1)} - \frac{y}{\bar{y}(\bar{x}\bar{y} + 1)}, \tag{27}$$

$\forall x > 0, \bar{x} > 0, y > 0, \bar{y} > 0.$

Let i denote the ith iteration and exploit

$$x_1 = \frac{1}{P_0\, p_{0,k}|\rho_{0,k,k}|^2}, \quad y_1 = \mathcal{I}_k^{\text{intra}}(\boldsymbol{p}_0) + \sigma_k^2,$$
$$\bar{x}_1 = x_1^{(i)} = \frac{1}{P_0\, p_{0,k}^{(i)}|\rho_{0,k,k}|^2}, \quad \bar{y}_1 = y_1^{(i)} = \mathcal{I}_k^{\text{intra}}(\boldsymbol{p}_0^{(i)}) + \sigma_k^2,$$

for the approximation of the kth PU's throughput in (11) as

$$R_{0,k}(\boldsymbol{p}_0, \boldsymbol{p}_M) \geq \hat{R}_{0,k}^{(i)}(\boldsymbol{p}_0, \boldsymbol{p}_M), \forall k \in \mathcal{K}_P \tag{28}$$

where

$$\hat{R}_{0,k}^{(i)}(\boldsymbol{p}_0, \boldsymbol{p}_M) = \ln\left(1 + \frac{1}{\bar{x}_1\bar{y}_1}\right) + \frac{2}{(\bar{x}_1\bar{y}_1 + 1)} - \frac{x_1}{\bar{x}_1(\bar{x}_1\bar{y}_1 + 1)} - \frac{y_1}{\bar{y}_1(\bar{x}_1\bar{y}_1 + 1)}. \tag{29}$$

Similarly, we can invoke

$$x_2 = \frac{1}{P_m|\rho_{m,0,m}|^2}, \quad y_2 = \mathcal{I}_m^{\text{MBS}}(\boldsymbol{p}_M) + \sigma_0^2,$$
$$\bar{x}_2 = x_2^{(i)} = \frac{1}{P_m^{(i)}|\rho_{m,0,m}|^2}, \quad \bar{y}_2 = y_2^{(i)} = \mathcal{I}_m^{\text{BS}}(\boldsymbol{p}_M^{(i)}) + \sigma_0^2,$$

for the approximation of BS's throughput function in (15) as

$$R_{m,0}(\boldsymbol{p}_M) \geq \hat{R}_{m,0}^{(i)}(\boldsymbol{p}_M), m \in \mathcal{M} \tag{30}$$

where

$$\hat{R}_{m,0}^{(i)}(\boldsymbol{p}_M) = \ln\left(1 + \frac{1}{\bar{x}_2\bar{y}_2}\right) + \frac{2}{(\bar{x}_2\bar{y}_2 + 1)} - \frac{x_2}{\bar{x}_2(\bar{x}_2\bar{y}_2 + 1)} - \frac{y_2}{\bar{y}_2(\bar{x}_2\bar{y}_2 + 1)}. \tag{31}$$

ACKNOWLEDGMENT
This article has been presented in part at the IEEE Global Communications Conference, December 9-13, 2019, Waikoloa, HI, USA.

REFERENCES

[1] T. Q. Duong, L. D. Nguyen, H. D. Tuan, and L. Hanzo, "Learning-aided realtime performance optimisation of cognitive UAV-assisted disaster communication," in *Proc. IEEE Global Commun. Conf. (GLOBECOM)*, Dec. 2019, pp. 1–6.
[2] L. D. Nguyen, A. Kortun, and T. Q. Duong, "An introduction of real-time embedded optimisation programming for uav systems under disaster communication," *EAI Endorsed Trans. Ind. Netw. Intell. Syst.*, vol. 5, no. 17, pp. 1–8, Dec. 2018.
[3] X. Liu, M. Guan, X. Zhang, and H. Ding, "Spectrum sensing optimization in an UAV-based cognitive radio," *IEEE Access*, vol. 6, pp. 44002–44009, 2018.
[4] L. Sboui, H. Ghazzai, Z. Rezki, and M.-S. Alouini, "Achievable rates of UAV-relayed cooperative cognitive radio MIMO systems," *IEEE Access*, vol. 5, pp. 5190–5204, 2017.
[5] L. Wang, H. Yang, J. Long, K. Wu, and J. Chen, "Enabling ultra-dense UAV-aided network with overlapped spectrum sharing: Potential and approaches," *IEEE Netw.*, vol. 32, no. 5, pp. 85–91, Sep. 2018.
[6] Y. Huang, J. Xu, L. Qiu, and R. Zhang, "Cognitive UAV communication via joint trajectory and power control," in *Proc. IEEE 19th Int. Workshop Signal Process. Adv. Wireless Commun. (SPAWC)*, Jun. 2018, pp. 1–5.
[7] L. Sboui, H. Ghazzai, Z. Rezki, and M.-S. Alouini, "Energy-efficient power allocation for UAV cognitive radio systems," in *Proc. IEEE 86th Veh. Technol. Conf. (VTC-Fall)*, Sep. 2017, pp. 1–5.
[8] Y. Zhou, F. Zhou, H. Zhou, D. W. K. Ng, and R. Q. Hu, "Robust trajectory and transmit power optimization for secure UAV-enabled cognitive radio networks," *IEEE Trans. Commun.*, vol. 68, no. 7, pp. 4022–4034, Jul. 2020.
[9] H. T. Nguyen, H. D. Tuan, T. Q. Duong, H. V. Poor, and W.-J. Hwang, "Joint D2D assignment, bandwidth and power allocation in cognitive UAV-enabled networks," *IEEE Trans. Cognit. Commun. Netw.*, vol. 6, no. 3, pp. 1084–1095, Sep. 2020.
[10] X. Liang, W. Xu, H. Gao, M. Pan, J. Lin, Q. Deng, and P. Zhang, "Throughput optimization for cognitive UAV networks: A three-dimensional-location-aware approach," *IEEE Wireless Commun. Lett.*, vol. 9, no. 7, pp. 948–952, Jul. 2020.
[11] Y. Huang, W. Mei, J. Xu, L. Qiu, and R. Zhang, "Cognitive UAV communication via joint maneuver and power control," *IEEE Trans. Commun.*, vol. 67, no. 11, pp. 7872–7888, Nov. 2019.
[12] M.-N. Nguyen, L. D. Nguyen, T. Q. Duong, and H. D. Tuan, "Real-time optimal resource allocation for embedded UAV communication systems," *IEEE Wireless Commun. Lett.*, vol. 8, no. 1, pp. 225–228, Feb. 2019.
[13] T. Q. Duong, L. D. Nguyen, and L. K. Nguyen, "Practical optimisation of path planning and completion time of data collection for UAV-enabled disaster communications," in *Proc. 15th Int. Wireless Commun. Mobile Comput. Conf. (IWCMC)*, Jun. 2019, pp. 1–5.
[14] R. I. Bor-Yaliniz, A. El-Keyi, and H. Yanikomeroglu, "Efficient 3-D placement of an aerial base station in next generation cellular networks," in *Proc. IEEE Int. Conf. Commun. (ICC)*, May 2016, pp. 1–5.
[15] M. Mozaffari, W. Saad, M. Bennis, and M. Debbah, "Efficient deployment of multiple unmanned aerial vehicles for optimal wireless coverage," *IEEE Commun. Lett.*, vol. 20, no. 8, pp. 1647–1650, Aug. 2016.
[16] A. Al-Hourani, S. Kandeepan, and S. Lardner, "Optimal LAP altitude for maximum coverage," *IEEE Wireless Commun. Lett.*, vol. 3, no. 6, pp. 569–572, Dec. 2014.
[17] T. L. Marzetta, E. G. Larsson, H. Yang, and H. Q. Ngo, *Fundamentals of Massive MIMO*. Cambridge, U.K: Cambridge Univ. Press, 2016.
[18] M. Alzenad, A. El-Keyi, and H. Yanikomeroglu, "3-D placement of an unmanned aerial vehicle base station for maximum coverage of users with different QoS requirements," *IEEE Wireless Commun. Lett.*, vol. 7, no. 1, pp. 38–41, Feb. 2018.
[19] S. Diamond and S. Boyd, "CVXPY: A Python-embedded modeling language for convex optimization," *J. Mach. Learn. Res.*, vol. 17, no. 83, pp. 1–5, 2016.

[20] Y. Chen, M. W. Hoffman, S. G. Colmenarejo, M. Denil, T. P. Lillicrap, and N. de Freitas, "Learning to learn for global optimization of black box functions," in *Proc. 30th Conf. Neur. Inf. Process. Syst.*, Barcelona, Spain, Dec. 2016, p. 18.
[21] H. Sun, X. Chen, Q. Shi, M. Hong, X. Fu, and N. D. Sidiropoulos, "Learning to optimize: Training deep neural networks for interference management," *IEEE Trans. Signal Process.*, vol. 66, no. 20, pp. 5438–5453, Oct. 2018.
[22] A. Cochocki and R. Unbehauen, *Neural Networks for Optimization and signal Processing*. New York, NY, USA: Wiley, 1993.
[23] I. Goodfellow, Y. Bengio, A. Courville, and Y. Bengio, *Deep Learning*. Cambridge, MA, USA: MIT Press, 2016, vol. 1.
[24] L. Deng and D. Yu, "Deep learning: Methods and applications," *Found. Trends Signal Process.*, vol. 7, nos. 3–4, pp. 197–387, Jun. 2014.
[25] L. D. Nguyen, H. D. Tuan, T. Q. Duong, O. A. Dobre, and H. V. Poor, "Downlink beamforming for energy-efficient heterogeneous networks with massive MIMO and small cells," *IEEE Trans. Wireless Commun.*, vol. 17, no. 5, pp. 3386–3400, May 2018.
[26] L. D. Nguyen, H. D. Tuan, T. Q. Duong, and H. V. Poor, "Multi-user regularized zero-forcing beamforming," *IEEE Trans. Signal Process.*, vol. 67, no. 11, pp. 2839–2853, Jun. 2019.

MINH-HIEN T. NGUYEN is currently pursuing the Ph.D. degree in electronics and electrical engineering with Queen's University Belfast, U.K. Her current research interests include wireless communications, UAV, real-time optimization, and machine learning.

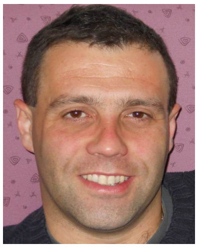

EMILIANO GARCIA-PALACIOS received the Ph.D. degree from Queen's University Belfast, in 2000. He is currently a Senior Lecturer with Queen's University Belfast. Since then, he has been leading research in wireless network resource management. His research interests include wireless protocols, wireless resource allocation and optimization, and traffic management for next generation gigabit networks.

TAN DO-DUY received the B.S. degree from the HCMC University of Technology (BK-HCM), Ho Chi Minh City, Vietnam, in 2010, the M.S. degree from the Kumoh National Institute of Technology, Gumi, South Korea, in 2013, and the Ph.D. degree from the Autonomous University of Barcelona, Barcelona, Spain, in 2019. He is currently a Lecturer with the Department of Computer and Communication Engineering, HCMC University of Technology and Education. His main research interests include wireless cooperative communications and network coding applications for wireless networking.

LONG D. NGUYEN (Member, IEEE) received the Ph.D. degree in electronics and electrical engineering from Queen's University Belfast (QUB), U.K., in 2018. He was a Research Fellow with Queen's University Belfast, for a part of Newton Project, from 2018 to 2019. He is currently an Assistant Professor with Dong Nai University, Vietnam, and an Adjunct Assistant Professor with Duy Tan University. His research interests include convex optimization techniques for resource management in wireless communications, energy efficiency approaches (heterogeneous networks, relay networks, cell-free networks, and massive MIMO), and real-time embedded optimization for wireless networks and the Internet of Things (IoTs).

SON T. MAI is currently an Assistant Professor with Queen's University Belfast, U.K. Before, he was with the University of Grenoble Alpes, France, Aarhus University, Denmark, and Ludwig-Maximilians University of Munich (LMU), Germany. His research interests include machine learning and data mining algorithms for large complex data.

TRUNG Q. DUONG (Senior Member, IEEE) is currently a Professor and the Chair of Telecommunications with Queen's University Belfast, U.K., and a Research Chair with the Royal Academy of Engineering. His current research interests include wireless communications, signal processing, and machine learning. He was awarded the Best Paper Award from the IEEE Vehicular Technology Conference (VTC-Spring), in 2013, the IEEE International Conference on Communications (ICC), in 2014, the IEEE Global Communications Conference (GLOBECOM), in 2016, the IEEE Digital Signal Processing Conference (DSP), in 2017, and GLOBECOM, in 2019. He was a recipient of the prestigious Royal Academy of Engineering Research Fellowship, from 2015 to 2020, and has won a prestigious Newton Prize, in 2017. He currently serves as an Editor for the IEEE Transactions on Wireless Communications.